

# Active Sensing Acousto-Ultrasound SHM via Stochastic Non-Stationary Time Series Models

Shabbir Ahmed and Fotis Kopsaftopoulos

Intelligent Structural Systems Laboratory (ISSL), Mechanical, Aerospace and Nuclear Engineering, Rensselaer Polytechnic Institute, Troy, NY 12180, USA  
`{ahmeds6,kopsaf}@rpi.edu`

**Abstract.** In this work, a novel statistical approach for damage detection and identification in the context of ultrasonic guided wave-based damage diagnosis is proposed using stochastic functional series time-varying autoregressive (FS-TAR) models. Wavelet functions are used as the functional basis family and the coefficients of projection of the time-varying model parameters are estimated via a maximum likelihood scheme. Damage detection and identification are tackled within a statistical decision making framework while appropriate thresholds are derived using pre-determined type I error probability levels. Both damage intersecting and non-intersecting, with respect to wave propagation, paths are considered in a multi-sensor aluminum plate in pitch-catch configuration. The method's robustness, effectiveness, and limitations are discussed. The results indicate the effectiveness of the proposed method in detecting and identifying damage within a statistical setting.

**Keywords:** Damage detection · structural health monitoring · guided waves · time varying models · time series models · FS-TAR models

## 1 Introduction

Ultrasonic guided waves are elastic stress waves that propagate through thin structures and have been extensively used in the field of structural health monitoring (SHM) for detecting structural damage [1]. They are highly sensitive and effective at detecting different types of damage, such as cracks, corrosion, delamination, etc., in mechanical and aerospace structures. Guided-waves SHM methods are capable of monitoring large structural areas due to the ability of the waves to propagate long distances without much dissipation [3]. In addition, guided waves can be easily generated/detected by piezoelectric transducers in the form of an applied strain/voltage from the surface of the structure [1, 13].

In the context of active sensing guided-waves SHM, the most common metrics for detecting damage are based on the concept of damage index (DI), where features of the guided wave signal, such as the time of flight (ToF), specific mode signal amplitude, spectral properties and signal energy for an unknown structural state are compared to that of the healthy state of the structure [1]. In addition to time domain DIs, the use of frequency domain or combined time-frequency domain expressions has been reported [6, 5]. However, the majority

of the DI formulations in the literature are deterministic and require a user defined detection and identification threshold. Recently, steps have been taken towards formulating probabilistic DIs using Gaussian mixture models, Gaussian process regression and other probabilistic or statistical tools [1, 12, 4]. For the case of the Gaussian mixture models, instead of comparing the individual healthy and damaged state DIs, their probability distributions are compared via the Kullback-Liebler (KL) divergence or appropriate modifications [12]. However, such probabilistic DI-based formulations may show suboptimal performance if the reflections part of the guided wave signal is included in the analysis. In addition, these methods do not model the actual wave propagation for different paths nor account for the underlying wave propagation dynamics.

In order to address these issues and improve the performance of the existing guided wave-based damage detection and identification frameworks, stochastic time series models are used in the present study to formulate a statistical SHM method for active sensing SHM. These models are capable of capturing the underlying dynamics of wave propagation, are inherently accounting for uncertainty, and are statistical in nature therefore allowing for the formalization of decision making schemes via the use of statistical hypothesis testing under predetermined type I error probability levels. Stochastic time series models have been extensively used in the context of vibration-based SHM [8, 2, 7]. As guided waves are non-stationary signals with dispersive characteristics and time-varying variance, time-varying parametric time series models are required for their effective representation. Time-varying parametric methods can be based upon parameterized representations of the time-dependent auto-regressive moving average (TARMA) or related types and their extensions. Such representations differ from their conventional, stationary, counterparts in that their parameters are time dependent [10, 15].

The main objective of this work is the introduction and experimental assessment of a novel damage detection and identification scheme for active sensing SHM based on functional-series time-varying autoregressive (FS-TAR) models. These models are used to represent the guided wave propagation for different actuator-sensor paths on the monitored structure and the estimated time-varying parameters are subsequently used to tackle damage detection and identification within a statistical hypothesis decision making scheme. The parameters of the FS-TAR model are projected onto functional subspaces assuming a deterministic evolution of the wave propagation. The family of basis functions selected for the projection of the FS-TAR model's time-dependent parameters is of crucial importance. By taking advantage of prior information about the physics of the non-stationary signals or parameter evolution, appropriate families of basis functions (wavelets, trigonometric, polynomial, etc.) can be selected. As guided wave propagation is deterministic in nature for a specific structure, geometry, material properties and boundary conditions, FS-TAR representations constitute a natural choice. Both the coefficients of projection (COP) and the time-varying parameters are used for damage diagnosis. To the authors' best of knowledge,

this is the first study that explores the use of stochastic time-varying time series models in the context of active sensing acousto-ultrasound-based SHM.

## 2 Stochastic Identification and Damage Detection

Guided waves are inherently non-stationary due to their time-dependent (evolutionary) characteristics. Deterministic parameter evolution TAR representation imposes deterministic structure upon the time evolution of their parameters [10]. This is achieved by postulating model parameters as deterministic functions of time, belonging to specific functional subspaces. Such representations are referred to as FS-TAR models. Their AR parameters, as well as innovations standard deviation, are all expanded within properly selected functional subspaces defined as

$$\mathcal{F}_{AR} \triangleq \{G_{b_a(1)}[t], G_{b_a(2)}[t] \dots G_{b_a(p_a)}[t]\} \quad (1)$$

$$\mathcal{F}_{\sigma_e} \triangleq \{G_{b_s(1)}[t], G_{b_s(2)}[t] \dots G_{b_s(p_s)}[t]\} \quad (2)$$

In these expressions, the “ $\mathcal{F}$ ” designates the functional subspace of the indicating quantity and  $G_j[t]$  a set of orthogonal basis functions selected from a suitable family (such as Chebyshev, Legendre, other polynomials, trigonometric, wavelet or other functions). The AR and standard deviation subspace dimensionalities are indicated as  $p_a$  and  $p_s$ , respectively, while, the indices  $b_a(i)(i = 1, \dots, p_a)$  and  $b_s(i)(i = 1, \dots, p_s)$  designate the specific basis functions of a particular family that are included in each subspace. The time-dependent AR and innovations standard deviations of an FS-TAR( $na$ ) $_{[p_a, p_s]}$  representation may thus be expressed as

$$y[t] + \sum_{i=1}^{na} a_i[t] \cdot y[t-i] = e[t], \quad \text{with } e[t] \sim \text{iid } \mathcal{N}(0, \sigma_e^2[t]) \quad (3)$$

$$a_i[t] \triangleq \sum_{j=1}^{p_a} a_{i,j} \cdot G_{b_a(j)}[t] \quad \sigma_e[t] \triangleq \sum_{j=1}^{p_s} s_j \cdot G_{b_s(j)}[t] \quad (4)$$

with  $a_{i,j}$  and  $s_j$  designating the AR and innovations standard deviation coefficients of projection. An FS-TAR model is thus parametrized in terms of its projection coefficients  $a_{i,j}$  and  $s_j$ . The coefficients of projection vector

$\boldsymbol{\theta} = [a_{1,1} \dots a_{1,p_a} : \dots : a_{na,1} \dots a_{na,p_a}]^T_{[napax1]}$  has to be estimated from the available data.

The model identification problem for FS-TAR is usually distinguished into two subproblems: (i) *parameter estimation* and (ii) *model structure selection*. For a detailed review of parameter estimation and model structure selection methods see [10, 9].

The maximum likelihood (ML) estimation of the coefficients of projection vector  $\boldsymbol{\theta}$  may be obtained through the maximization of the log-likelihood function, which for the FS-TAR model and under the Gaussian assumption for the innovations sequence may be given as

$$\ln \mathcal{L}(\boldsymbol{\vartheta}, \boldsymbol{\sigma}_e | y^N) = -\frac{N}{2} \ln 2\pi - \frac{1}{2} \sum_{t=1}^N \left( \ln \sigma_e^2[t] + \frac{e^2[t, \boldsymbol{\vartheta}]}{\sigma_e^2[t]} \right) \quad (5)$$

with  $\boldsymbol{\sigma}_e = [\sigma_e^2[1], \dots, \sigma_e^2[N]]^T$  constituting a nuisance parameter vector of high dimensionality while  $\boldsymbol{\vartheta}$  is a parameter vector of low dimensionality. In such cases, the nuisance parameter vector may be profiled out from the log-likelihood function by considering the conditional maximum likelihood (CML) estimate of  $\hat{\sigma}_e$  for known  $\boldsymbol{\vartheta}$  and substituting it into Equation 5. Towards this end,

$$\frac{\partial \ln \mathcal{L}}{\partial \sigma_e^2[t]} = 0 \implies -\frac{1}{2} \cdot \left[ \frac{1}{\sigma_e^2[t]} - \frac{e^2[t, \boldsymbol{\vartheta}]}{\sigma_e^4[t]} \right] \implies \hat{\sigma}_e^2[t] = e^2[t, \boldsymbol{\vartheta}] \quad (6)$$

Then it follows that

$$\hat{\boldsymbol{\vartheta}} = \arg \max_{\boldsymbol{\vartheta}} \{\ln \mathcal{L}(\boldsymbol{\vartheta}, \hat{\sigma}_e | y^N)\} = \arg \max_{\boldsymbol{\vartheta}} \left[ -\frac{1}{2} \sum_{t=1}^N \ln e^2[t, \boldsymbol{\vartheta}] \right] \quad (7)$$

$\hat{\boldsymbol{\vartheta}}$  is actually a pseudo-likelihood estimator which actually leads to the same point estimate with the original ML estimator of  $\boldsymbol{\vartheta}$  and  $\boldsymbol{\sigma}_e$ . Once the FS-TAR coefficients of projection vector  $\boldsymbol{\vartheta}$  is estimated (which are constants), the time-varying parameter vector  $\boldsymbol{\theta}[t] = [a_1[t], a_2[t] \dots a_{na}[t]]_{nax1}$  can be estimated by multiplying with the basis functions as shown in Equation 4. The estimation of the innovations standard deviation coefficients of projection may be achieved as described in [14]. For details of the FS-TAR model structure selection see [10, 11, 14].

In this study, damage detection and identification have been performed in two different ways: (a) using coefficients of projection which provides damage diagnosis results similar to the AR models; (b) using time-varying model parameters which provides time-varying damage diagnosis.

## 2.1 Coefficients of Projection-based Damage Diagnosis

In this method, damage detection and identification of a structure can be based on a characteristic quantity  $Q = f(\boldsymbol{\vartheta})$ , which is a function of the AR coefficients of projection vector  $\boldsymbol{\vartheta}$  of the FS-TAR model. Note that coefficients of projection are constants and do not vary with time. Let  $\hat{\boldsymbol{\vartheta}}$  designate a proper estimator of the coefficients of projection vector  $\boldsymbol{\vartheta}$ . For a sufficiently long signal, the estimator is (under mild assumptions) Gaussian distributed with mean equal to its true value  $\boldsymbol{\vartheta}$  and a certain covariance  $\mathbf{P}_{\boldsymbol{\vartheta}}$ , hence  $\hat{\boldsymbol{\vartheta}} \sim \mathcal{N}(\boldsymbol{\vartheta}, \mathbf{P}_{\boldsymbol{\vartheta}})$ . Damage diagnosis is then based on testing for statistically significant changes in the coefficients of projection vector  $\boldsymbol{\vartheta}$  between the nominal and current state of the structure through the following hypothesis testing problem:

$$H_0 : \delta\boldsymbol{\vartheta} = \boldsymbol{\vartheta}_o - \boldsymbol{\vartheta}_u = 0 \quad \text{null hypothesis--healthy structure} \quad (8)$$

$$H_1 : \delta\boldsymbol{\vartheta} = \boldsymbol{\vartheta}_o - \boldsymbol{\vartheta}_u \neq 0 \quad \text{alternative hypothesis -- damaged structure} \quad (9)$$

The difference between the two parameter vector estimators follows Gaussian distribution, that is,  $\delta\widehat{\boldsymbol{\vartheta}} = \widehat{\boldsymbol{\vartheta}}_o - \widehat{\boldsymbol{\vartheta}}_u \sim \mathcal{N}(\delta\widehat{\boldsymbol{\vartheta}}, \delta\mathbf{P}_{\boldsymbol{\vartheta}})$ , with  $\delta\boldsymbol{\vartheta} = \boldsymbol{\vartheta}_o - \boldsymbol{\vartheta}_u$  and  $\delta\mathbf{P} = \mathbf{P}_o + \mathbf{P}_u$ , where  $\mathbf{P}_o, \mathbf{P}_u$  designate the corresponding covariance matrices. Under the null ( $H_0$ ) hypothesis  $\delta\widehat{\boldsymbol{\vartheta}} = \widehat{\boldsymbol{\vartheta}}_o - \widehat{\boldsymbol{\vartheta}}_u \sim \mathcal{N}(0, 2\mathbf{P}_o)$  and the quantity

$$Q = \delta\widehat{\boldsymbol{\vartheta}}^T \cdot \delta\mathbf{P}^{-1} \cdot \delta\widehat{\boldsymbol{\vartheta}}, \quad \delta\mathbf{P} = 2\mathbf{P}_o \quad (10)$$

follows a  $\chi^2$  distribution with  $d = \dim(\boldsymbol{\vartheta})$  (parameter vector dimensionality) degrees of freedom. As the covariance matrix  $\mathbf{P}_o$  corresponding to the healthy structure is unavailable, its estimated version  $\widehat{\mathbf{P}}_o$  is used. It is to be noted here that, when  $\widehat{\mathbf{P}}_o$  is estimated from the data, the quantity  $Q$  in Equation 10 follows a Hotelling's  $\mathcal{T}^2$  distribution, which in turn, can be related to the Fisher's  $\mathcal{F}$  distribution. When  $N \rightarrow \infty$ , the  $\mathcal{F}$  distribution converges to  $\chi^2$  distribution. Then the following test is constructed at the  $\alpha$  (type I) risk level:

$$Q \leq \chi_{1-\alpha}^2(d) \implies H_0 \text{ is accepted} \quad (11)$$

$$\text{Else} \implies H_1 \text{ is accepted} \quad (12)$$

where,  $\chi_{1-\alpha}^2(d)$  designates the  $\chi^2$  distribution's  $(1 - \alpha)$  critical points. Damage identification may be based on a multiple hypothesis testing problem comparing the parameter vector  $\widehat{\boldsymbol{\vartheta}}_u$  belonging to the current structural state to those corresponding to different damage types  $\widehat{\boldsymbol{\vartheta}}_A, \widehat{\boldsymbol{\vartheta}}_B, \dots$

## 2.2 Time-varying Parameter-based Damage Diagnosis

In this method, damage diagnosis of a structure is based on a time-dependent characteristic quantity  $Q[t] = f(\boldsymbol{\theta}[t])$ , which is a function of the time-varying parameter vector  $\boldsymbol{\theta}[t]$  of the FS-TAR model. Here, note the incorporation of the time-dependent quantities. The associated time-varying damage detection and identification can be achieved in the similar way as mentioned in Section 2.1.

## 3 The Experimental Setup and the Signals

In this study, a  $152.4 \times 279.4$  mm ( $6 \times 11$  in) 6061 aluminum coupon (2.36 mm/0.093 in thick) was used (Figure 1(a)). Using Hysol EA 9394 adhesive, six lead zirconate titanate (PZT) piezoelectric sensors (type PZT-5A, Acellent Technologies, Inc) of 6.35 mm (1/4 in) diameter and a thickness of 0.2 mm (0.0079 in), were attached to the plate and cured for 24 hrs in room temperature. Figure 1(b) shows the dimensions of the plate, placement of the PZT transducers, and the path naming convention. Up to four three-gram weights were taped to the surface of the plate starting from its center point to simulate local damage (Figure 1(b)).

Actuation signals in the form of 5-peak tone bursts (5-cycle Hamming-filtered sine wave, 90 V peak-to-peak, 250 kHz center frequency) were generated in a pitch-catch configuration over each sensor consecutively. Data was collected using a ScanGenie III data acquisition system (Acellent Technologies, Inc) from

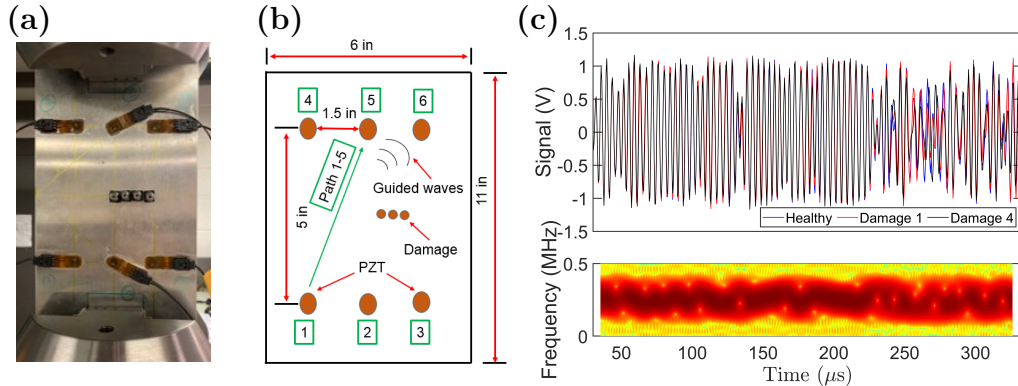


**Fig. 1.** (a) The aluminum plate used in this study with simulated damage; (b) a schematic of the plate's sensor layout and dimensions; (c) realization of the guided wave signal for healthy and damaged cases with a representative non-parametric spectrogram analysis.

selected sensors during each actuation cycle at a sampling frequency of 24 MHz. 20 signals for each sensor path (wave propagation path) and damage condition were recorded. This led to a total of 410 data sets. For the time-series modeling, the acquired signals were down-sampled to 2 MHz. This process resulted in 612-sample-long signals. Figure 1(c) presents an indicative non-parametric spectrogram analysis of the acquired signal<sup>1</sup>.

#### 4 Results and Discussions

Model selection of FS-TAR involves selecting the appropriate AR order  $na$  and functional subspaces  $\mathcal{F}_{AR}$  and  $\mathcal{F}_{\sigma_e}$ . In the present case, the best FS-TAR model minimizes the BIC criteria utilizing a suboptimal model selection method. At first, model order  $na$  is determined by considering a range of  $na$  values with an extended basis function dimensionality. In the present case,  $na = 2$  to  $na = 10$  was considered. The AR and variance subspace dimensionality  $pa$  and  $ps$  were 10 with consecutive wavelet basis functions. The model order  $na = 4$  was selected to be the best model order. Once the  $na = 4$  was selected, then the variance subspace dimensionality was kept constant and AR subspace dimensionality was varied. This resulted in the AR basis function dimensionality. The process was repeated for determining the variance basis function dimensionality [10, 14].

In this study, the functional subspace considered is wavelet basis function. For path 2-6 (damage intersecting path), the best model occurred for  $na = 4$  and the functional subspaces are  $\mathcal{F}_{AR} = \{G_1[t], G_2[t], G_3[t], G_4[t]\}$  ( $pa = 4$ ) and  $\mathcal{F}_{\sigma_e} = \{G_1[t], G_2[t]\}$  ( $ps = 2$ ). This is compactly written as FS-TAR(4)<sub>[4,2]</sub>. Similarly, for path 1-4 (damage non-intersecting path), the best model occurred

<sup>1</sup> window length: 30 samples; 98% overlap; NFFT points: 30000 (zero-padding took place to obtain smooth magnitude estimates); frequency resolution  $\Delta f = 666.66$  Hz.

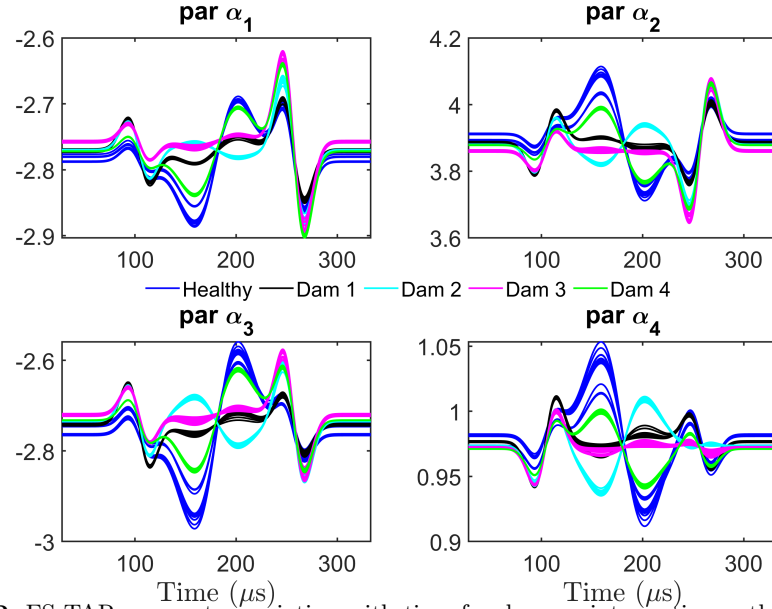


**Fig. 2.** FS-TAR parameter variation with time for damage intersecting path 2-6: parameters from all 5 states, namely: healthy, damage level 1, damage level 2, damage level 3 and damage level 4 have been plotted together for all 100 signals for all the four time-varying parameters.

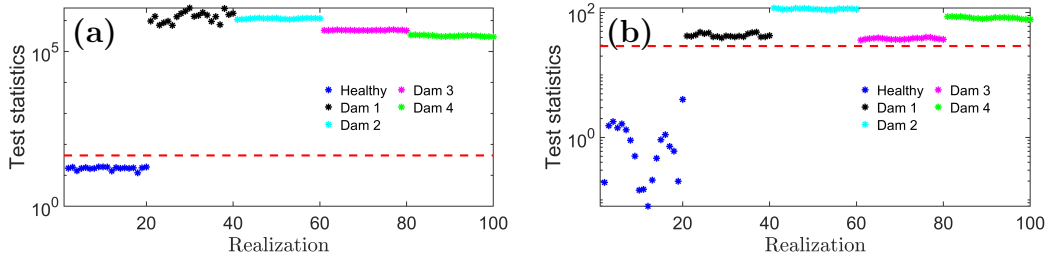


**Fig. 3.** Damage detection performance of the FS-TAR model using coefficients of projection of the wavelet basis function for damage intersecting path 2-6: (a) using the covariance matrix derived from 20 experimental healthy signals, and (b) FS-TAR(4)<sub>[4,2]</sub>-based covariance.

for  $na = 4$  and  $\mathcal{F}_{AR} = \{G_1[t], G_2[t], G_3[t], G_4[t], G_5[t]\}$  ( $pa = 5$ ) and  $\mathcal{F}_{\sigma_e} = \{G_1[t], G_2[t], G_3[t]\}$  ( $ps = 3$ ) compactly written as FS-TAR(4)<sub>[5,3]</sub>.

Figure 2 shows the time-varying model parameters of FS-TAR(4)<sub>[4,2]</sub> model for damage intersecting path 2-6. In this case, model parameters from different states have been plotted together for 100 experimental signals. It can also be observed that the model parameters of the same states are clustered together. Figure 3 shows the damage detection performance of the FS-TAR model using the coefficients of projection (COP) for damage intersecting path 2-6. In this

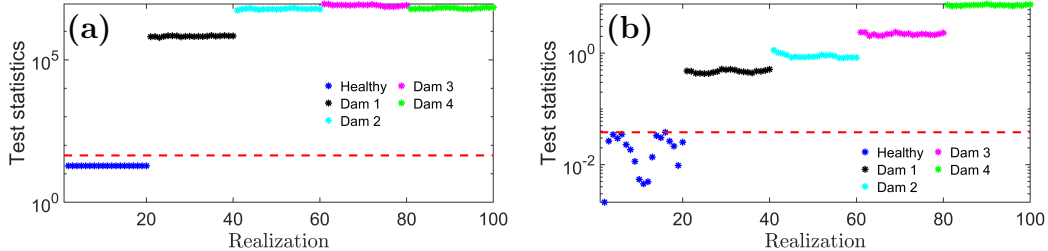


**Fig. 4.** Damage detection performance of the FS-TAR model using coefficients of projection of the wavelet basis function for damage non-intersecting path 1-4: (a) using the covariance matrix derived from 20 experimental healthy signals, and (b) FS-TAR(4)[5,3]-based covariance.

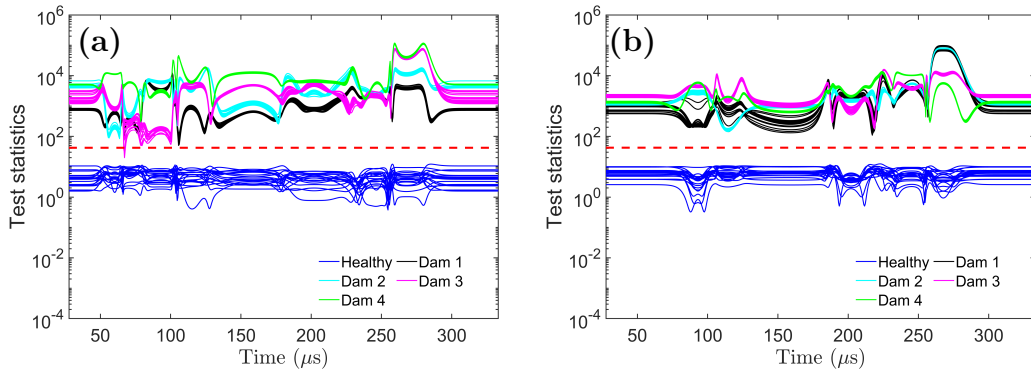


**Fig. 5.** Time-varying damage detection performance of the FS-TAR model using the wavelet basis functions and the experimental covariance: (a) for damage non-intersecting path 1-4, and (b) damage intersecting path 2-6.

case, the model has 16 COP and thus, the degrees of freedom  $d = 16$ . The dotted red line is the critical value of the characteristic quantity  $Q$  for  $\alpha = 0.001$  for the experimental case and  $\alpha = 0.03$  for the theoretical case (model based), with a degrees of freedom  $d = 16$ . Note that perfect damage detection was achieved and there is no missed damage for both using the experimental covariance as well as the FS-TAR(4)[4,2]-based covariance. Similarly, Figure 4 shows the damage detection performance of the FS-TAR(4)[5,3] model for damage non-intersecting path 1-4 using the experimental as well as FS-TAR(4)[4,2]-based covariance matrix. In this case too, perfect damage detection was achieved for both cases. The  $\alpha$ -level used for the experimental case was  $\alpha = 0.001$  for the damage non-intersecting path 1-4. For the theoretical case, the  $\alpha$ -level was manually adjusted.

Figure 5(a) shows the time-varying damage detection performance of the damage non-intersecting path 1-4 using FS-TAR(4)[5,3] model and Figure 5(b) shows the same for damage intersecting path 2-6 using FS-TAR(4)[4,2] model. For both cases, the experimental covariance matrix was used. Note that for all time instants, the healthy test statistics remain within the threshold (the dotted

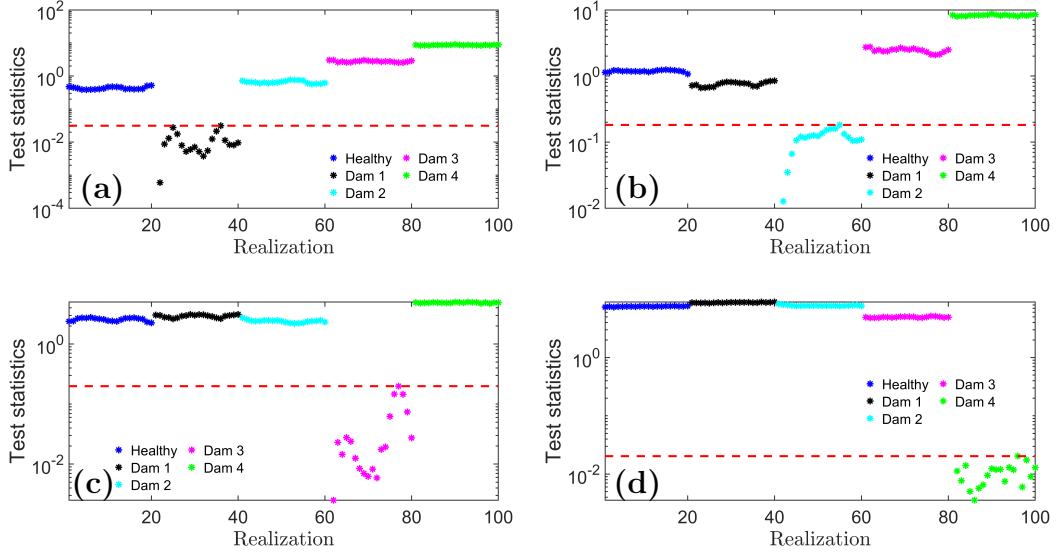


**Fig. 6.** Damage identification results for the damage non-intersecting path 1-4 using the coefficients of projection and FS-TAR(4)<sub>[5,3]</sub> model-based covariance matrix: identification of (a) damage level 1; (b) damage level 2; (c) damage level 3; (d) damage level 4.

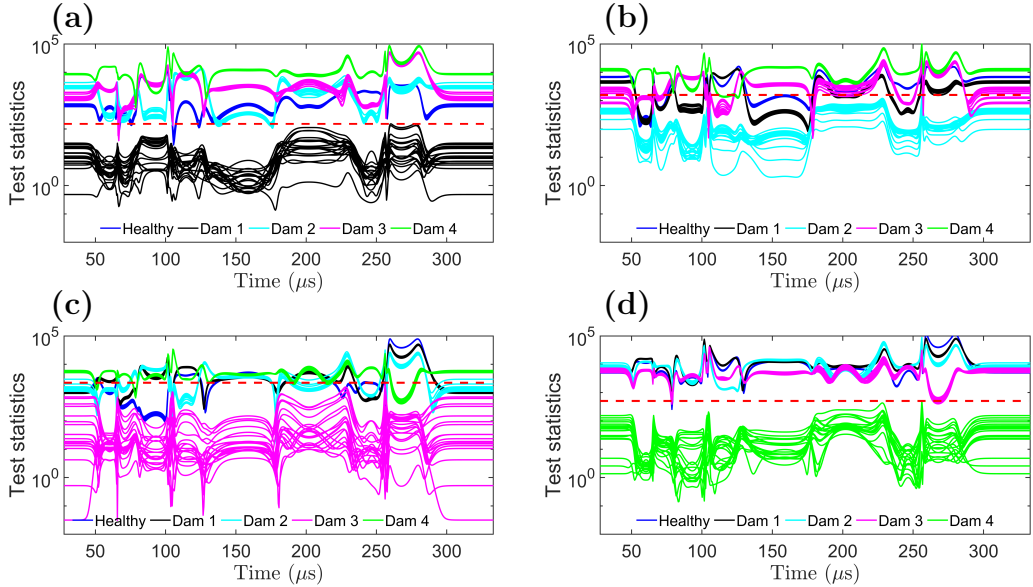
red line), and all the damaged states cross the threshold. The  $\alpha$ -level used was  $\alpha = 0.001$  for both cases.

Figure 6 shows the damage identification results of the four different damage states for damage non-intersecting path 1-4 using the FS-TAR(4)<sub>[5,3]</sub> model-based covariance matrix. Coefficients of projection (COP) were utilized in this case. Note that perfect identification was achieved for each damage state. The  $\alpha$  levels were manually adjusted in this case.

Figure 7 shows the time-varying damage identification results of the four different damage states for damage non-intersecting path 1-4 using the FS-TAR(4)<sub>[5,3]</sub> model-based time-varying parameters and the covariance matrix derived from 20 experimental healthy realizations. Note that perfect time-varying identification was achieved for each damage state. As for example, in Figure 7(a), only the damage level 1 lies below the threshold (dotted red line) for all time instants, whereas all other states cross the threshold. The healthy state has been shown here to demonstrate that simultaneous damage detection and identification is possible using the FS-TAR model.

## 5 Conclusions

The objective of this work is the formulation and numerical assessment of a statistical time-varying damage diagnosis scheme in the context of ultrasonic guided wave-based damage diagnosis using FS-TAR models. In the FS-TAR formulation, model parameters evolve in a deterministic way. These are output-only



**Fig. 7.** Time-varying damage identification results for the damage non-intersecting path 1-4 using the FS-TAR(4)<sub>[5,3]</sub> model-based time-varying model parameters and the experimental covariance matrix: identification of (a) damage level 1; (b) damage level 2; (c) damage level 3; (d) damage level 4.

methods and are capable of operating with a minimal number of guided wave response signals which may be of limited time duration and frequency bandwidth. These models have the potential to diagnose damage in an automated way. In general, it is difficult to detect and identify damage within a structure for damage non-intersecting paths. It was found that FS-TAR models are capable of detecting damage both for damage intersecting and non-intersecting paths using the experimental as well as FS-TAR-based covariance matrix.

The FS-TAR-based methods presented in the current paper for damage detection and identification of guided wave-based SHM are mathematically simple, computationally inexpensive, probabilistic in nature, and easy to use. In addition, these methods can potentially be automated with an aim of developing smart and intelligent structural systems.

## 6 Acknowledgments

This work was supported by the U.S. Air Force Office of Scientific Research (AFOSR) grant “Formal Verification of Stochastic State Awareness for Dynamic Data-Driven Intelligent Aerospace Systems” (FA9550-19-1-0054) and Program Officer Dr. Erik Blasch.

## References

1. Amer, A., Kopsaftopoulos, F.: Gaussian process regression for active sensing probabilistic structural health monitoring: Experimental assessment across multiple damage and loading scenarios. arXiv preprint arXiv:2106.14841 (2021)
2. Avendaño-Valencia, L.D., Chatzi, E.N., Koo, K.Y., Brownjohn, J.M.: Gaussian process time-series models for structures under operational variability. *Frontiers in Built Environment* **3**, 69 (2017)
3. Farrar, C.R., Worden, K.: An introduction to Structural Health Monitoring. *The Royal Society – Philosophical Transactions: Mathematical, Physical and Engineering Sciences* **365**, 303–315 (2007)
4. Haynes, C., Todd, M.D., Flynn, E., Croxford, A.: Statistically-based damage detection in geometrically-complex structures using ultrasonic interrogation. *Structural Health Monitoring* **12**(2), 141–152 (2013)
5. Hua, J., Cao, X., Yi, Y., Lin, J.: Time-frequency damage index of broadband lamb wave for corrosion inspection. *Journal of Sound and Vibration* **464**, 114985 (2020)
6. Jin, H., Yan, J., Li, W., Qing, X.: Monitoring of fatigue crack propagation by damage index of ultrasonic guided waves calculated by various acoustic features. *Applied Sciences* **9**(20), 4254 (2019)
7. Kopsaftopoulos, F.P., Fassois, S.D.: A stochastic functional model based method for vibration based damage detection, localization, and magnitude estimation. *Mechanical Systems and Signal Processing* **39**(1–2), 143–161 (August–September 2013)
8. Kopsaftopoulos, F., Fassois, S.: Vibration based health monitoring for a lightweight truss structure: experimental assessment of several statistical time series methods. *Mechanical Systems and Signal Processing* **24**(7), 1977–1997 (2010)
9. Ljung, L.: System identification: Theory for the user (1999)
10. Poulimenos, A., Fassois, S.: Parametric time-domain methods for non-stationary random vibration modelling and analysis—a critical survey and comparison. *Mechanical systems and signal processing* **20**(4), 763–816 (2006)
11. Poulimenos, A.G., Fassois, S.D.: Output-only stochastic identification of a time-varying structure via functional series tarma models. *Mechanical Systems and Signal Processing* **23**(4), 1180–1204 (2009)
12. Qiu, L., Fang, F., Yuan, S., Boller, C., Ren, Y.: An enhanced dynamic gaussian mixture model-based damage monitoring method of aircraft structures under environmental and operational conditions. *Structural Health Monitoring* **18**(2), 524–545 (2019)
13. Roy, S., Lonkar, K., Janapati, V., Chang, F.K.: A novel physics-based temperature compensation model for structural health monitoring using ultrasonic guided waves. *Structural Health Monitoring* **13**(3), 321–342 (2014)
14. Spiridonakos, M., Fassois, S.: An fs-tar based method for vibration-response-based fault diagnosis in stochastic time-varying structures: experimental application to a pick-and-place mechanism. *Mechanical Systems and Signal Processing* **38**(1), 206–222 (2013)
15. Spiridonakos, M., Fassois, S.: Non-stationary random vibration modelling and analysis via functional series time-dependent arma (fs-tarma) models—a critical survey. *Mechanical Systems and Signal Processing* **47**(1-2), 175–224 (2014)